Supplementary figures and tables

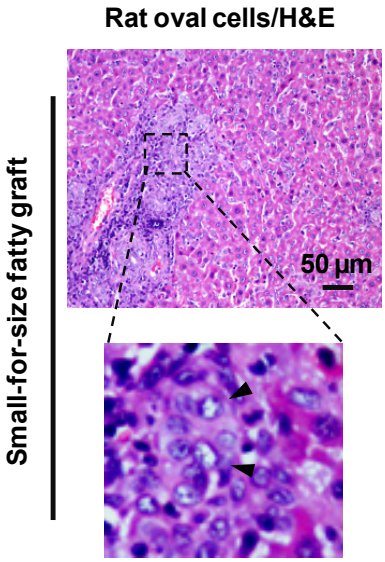

Figure S1. Proliferative hepatic progenitor cells (oval cells) in small-for-size fatty grafts. Histological examination showed that proliferative ductules in small-for-size fatty grafts composed of cells of small cytoplasm and poorly defined lumina (magnified figure, arrow).

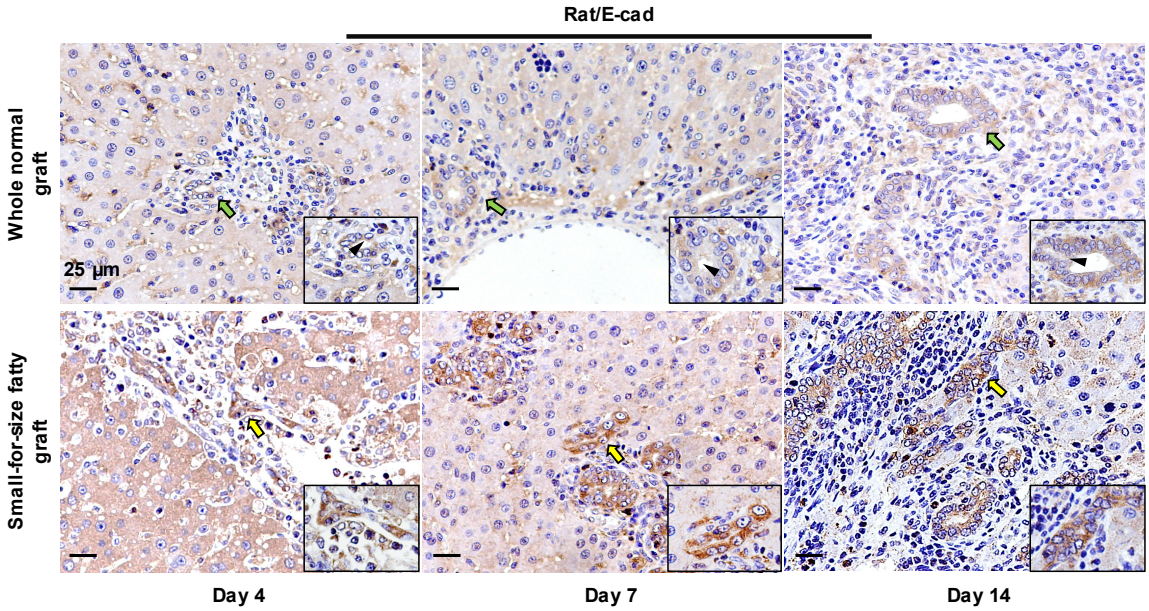

Figure S2. Whole membrane distribution of E-cadherin in small-for-size fatty liver grafts. Strong positivity for E-cadherin was observed on both the basolateral and apical membrane (whole cell membrane, insets in the lower panel) of most ductular cells in small-for-size fatty grafts. In contrast, expression of E-cadherin was limited to the basolateral membrane, being deficient on the apical side (insets in the upper panel, black arrows) in the whole normal grafts (n=6).

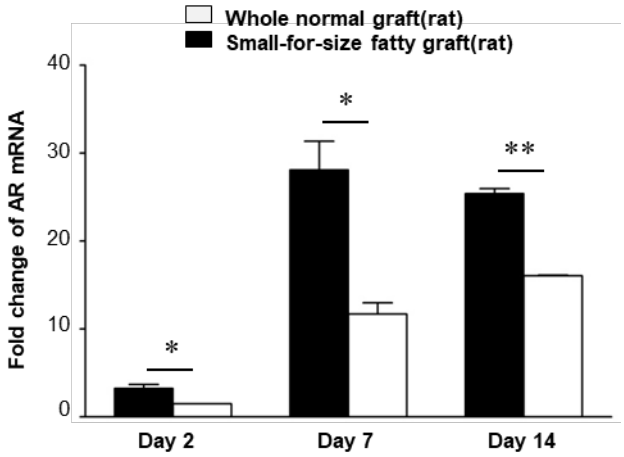

Figure S3. Increased mRNA level of AR in small-for-size fatty grafts. mRNA level of AR was significantly increased in small-for-size fatty graft compared with the whole normal graft (rat). ∗ $p<0.05$; ∗∗ $p<0.01$. Data represent the mean ± SD (n=6) and are representative of 2 independent experiments.

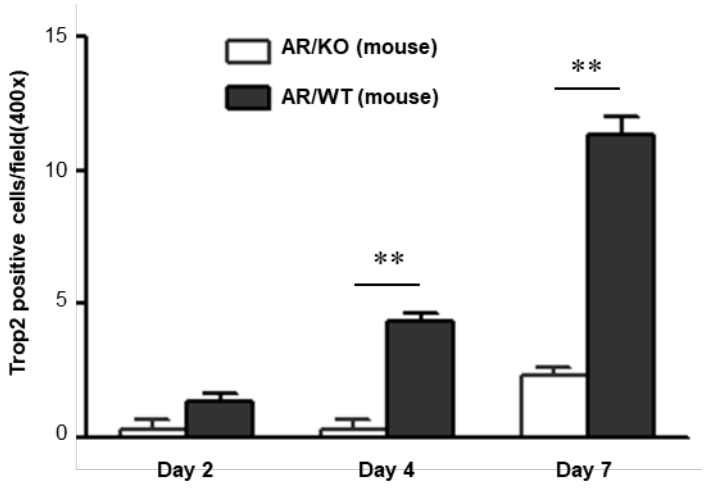

Figure S4. Oval cell activation in AR wild type mouse model. Statistical analysis of Trop2 positive cells in AR wild type or knock out mouse models under microscopic examination. Data represent the mean ± SD (n=6),∗∗ $p<0.01$.

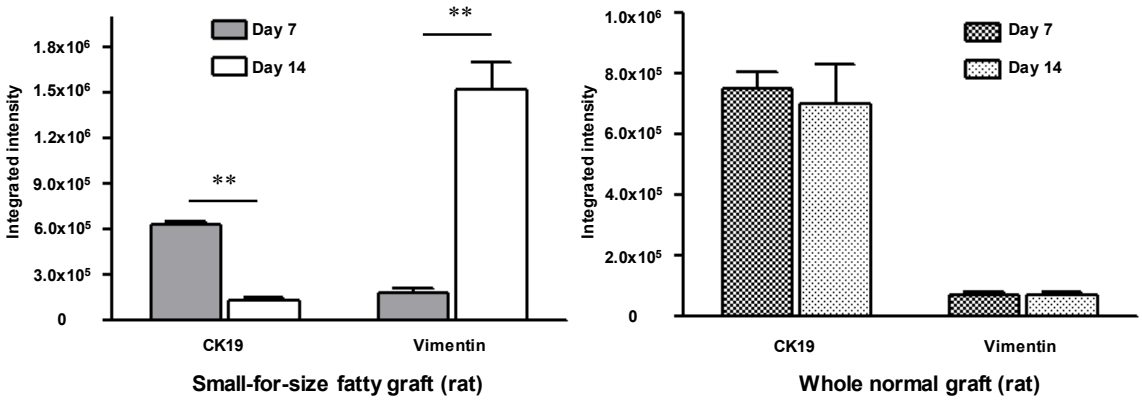

Figure S5. Dynamic alteration of CK19 and Vimentin in rat small-for-size fatty grafts. The expression levels of CK19 decreased while vimentin increased in biliary cells at day 14 post-transplantation compared with those at day 7 in the small-for-size fatty grafts (the integrated intensity of CK19 and Vimentin was analyzed by ImageJ after immunostaining).

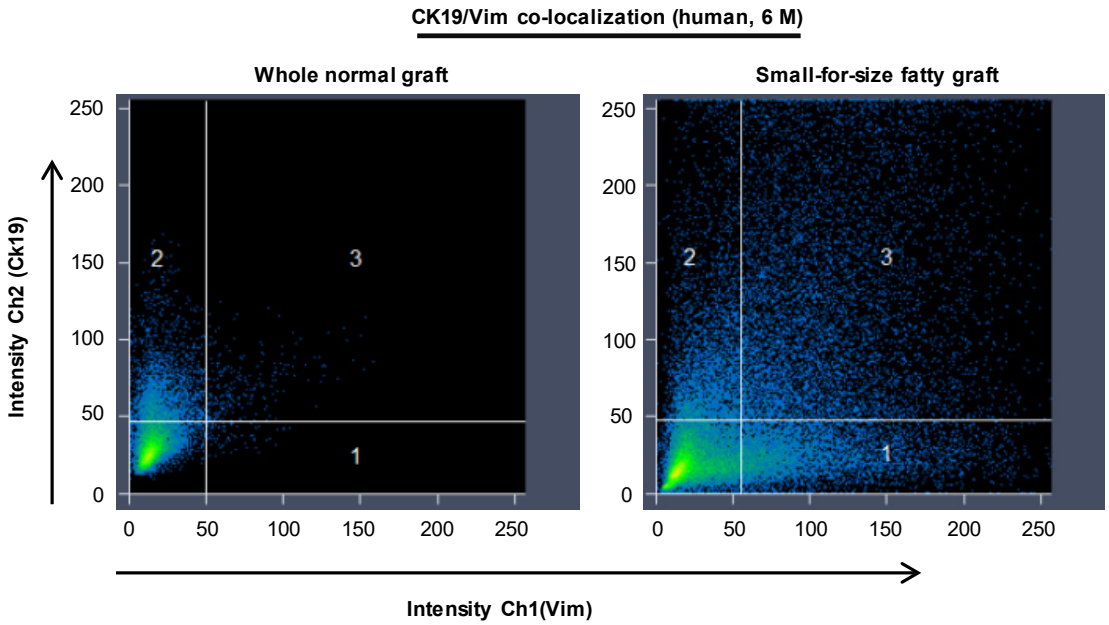

Figure S6. Co-localization of CK19 and vimentin in human small-for-size fatty grafts. Co-expression of CK19 and vimentin in reactive ductules of human small-for-size fatty graft (6 M) was revealed by co-localization analysis with ZEN under confocal microscopy.

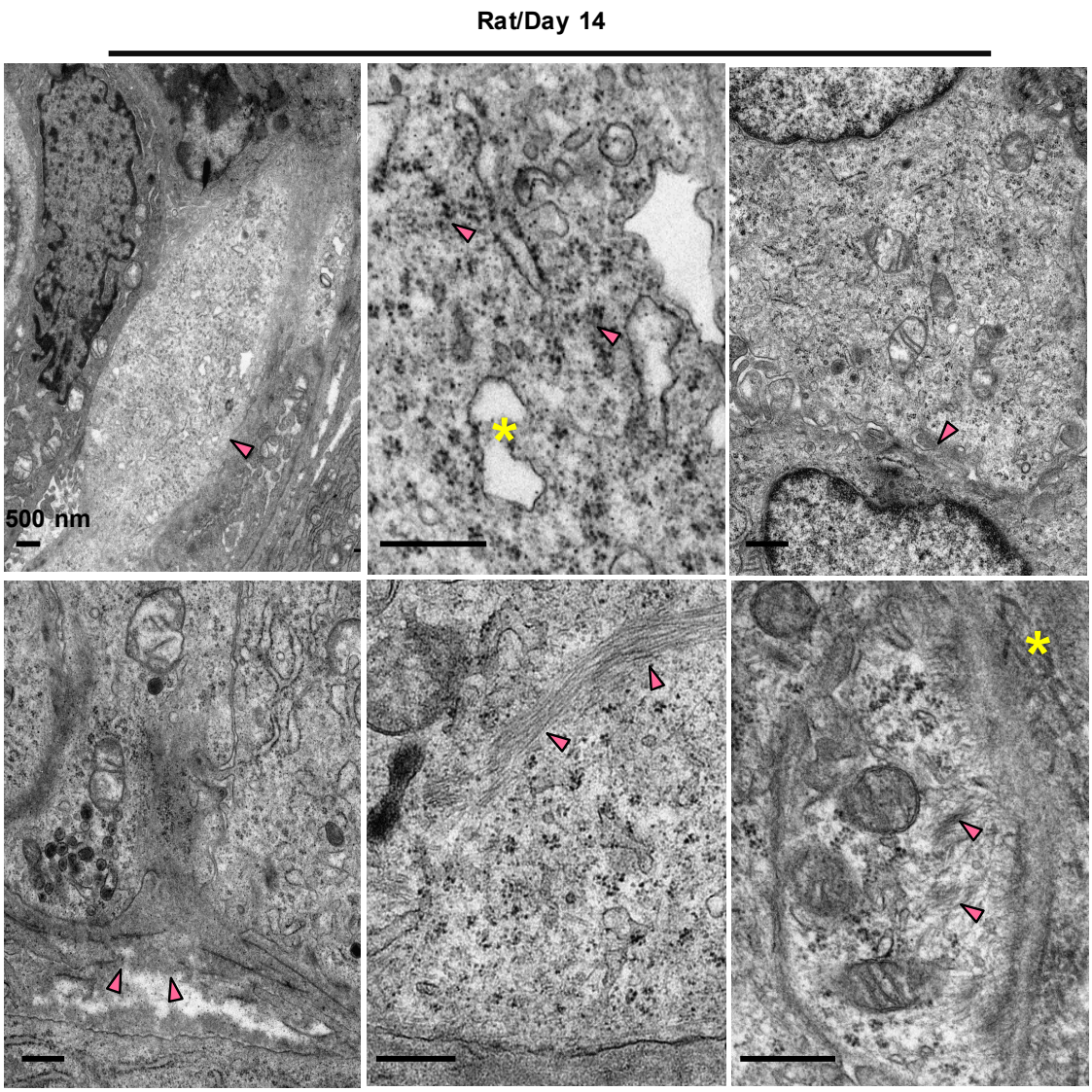

Figure S7. Proliferative biliary cells showing features of EMT under TEM in small-for-size fatty graft (rat). On day 14 after transplantation, the spindle-shaped biliary cells (left upper panel) showed well-developed endoplasmic reticulum (middle upper panel, asterisk) and ribosomes (middle upper panel, arrowhead) in the cytosol. Intercelluar junctions between biliary cells became partly disappeared at day 14 (right upper panel, arrowhead). Basement membrane was extensively damaged (left lower panel) and microfilaments were observed in the lateral or basal side (middle and right lower panels,

arrowhead) of biliary cells (adjacent collagen fibers in the basal side of biliary cells was indicated by asterisk).

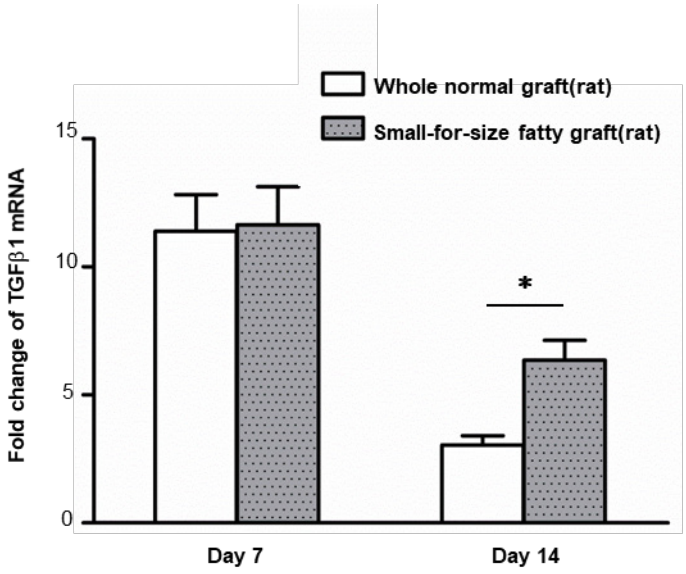

Figure S8. Enhanced expression of TGFβ-1 in small-for-size fatty grafts (rat). mRNA level of TGFβ-1 was enhanced after transplantation and the difference between small-for-size fatty graft and whole normal graft was significant at day 14. Data (normalized to normal liver) represent the mean ± SD (n=6) and are representative of 2 independent experiments. ∗ $p<0.05$.

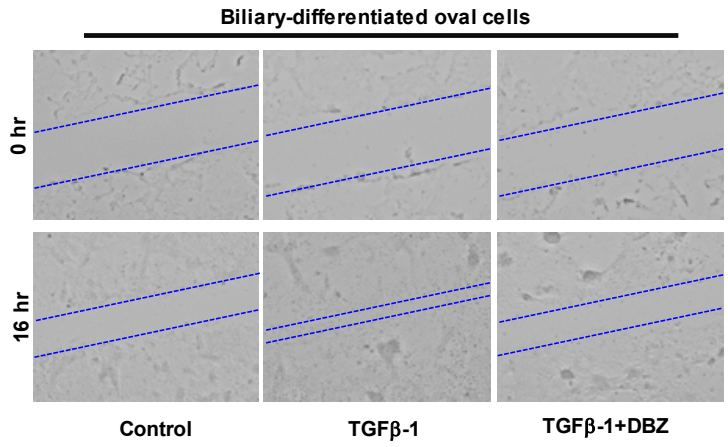

Figure S9. Attenuation of TGFβ1-induced cellular mobility by dibenzazepine (DBZ). Scratch assay showed that supplement of dibenzazepine (5 nM) for 16 hours suppressed mobility enhanced by TGFβ-1 in oval cell-derived biliary cells.

Table S1. Primers for qRT-PCR assessment.

Genes	Primer sequence
M[A]-CK7-F	5'-AGAGCCGGTTGTCTGGAGACGGAAT-3'
M-CK7-R	5'-ATGTGCTCAATTGTGGGTGCCCCT-3'
M-CK19-F	5'-AAGCCACCTACCTTGCTCGGATTG-3'
M-CK19-R	5'-ATCTGGATCTGCTCAGAGTGGACGG-3'
M-α SMA-F	5'-CTGTCAGGAACCCTGAGACGCT-3'
M-α SMA-R	5'-AGCATCATCACCAGCGAAGCCG-3'
M-Fibronectin-F	5'-AGCAAACGGCTGTCCCTCCT-3'
M-Fibronectin-R	5'-ACGGGTGAGTAGCGCACCAA-3'
M-collagen I α 1-F	5'-GAGCGGAGAGTACTGGATCG-3'
M-collagen I α 1-R	5'-GCTTCTTTTCCTTGGGGTTC-3'
M-Hes1-F:	5'-CCACGCTCCGCCACCATGAAG-3'
M-Hes1-R:	5'-GGCGCTTCTCGATGATGCCTCT-3'
M-Notch2-F	5'-TGTCTGTGCATGCCAGGTTT-3'
M-Notch2-R	5'-ATGTCGATCTGGCACACTGG-3'
M-E-cad-F	5'- CCACCAGATGACGATACCCG-3'
M-E-cad-R	5'- GAATCACTTCCGGTCTGGCA-3'
R[B]-AR-F:	5'-ATTCACTGGCCAACTGGCTT-3'
R-AR-R:	5'-GTTGCTCCATAGCCGTCCAA-3'

[A] M:mouse; [B] R:rat

Table S2. Primary antibodies for immunostaining or western blot.

Primary antibodies	Catalog Number	Sources
Aldose reductase	NBP1-00709	Novus Biologicals
OV6	MAB2020	R&D
CK19	M259	Bioworld
Vimentin	#2707-1	Epitomics
Laminin	NB300-144	Novus biologicals
Ki-67	556003	BD
Hes1	sc-166410	Santa cruz
Jag1	sc-8303	Santa cruz
E-cadherin	ab53033	Abcam
Trop2	sc-376181	Santa cruz
Cortactin	GTX100253	GeneTex
MT1-MMP	GTX61603	GeneTex
F-actin	A12379	Thermo Fisher
β-catenin	#8814	Cell signaling
CK7	ab9021	Abcam
Notch 2	SAB4502020	Sigma
MMP9	#3852	Cell signaling
ARPC2	PA5-21405	Thermo Fisher
CCND1	ab134175	Abcam
p27	#3688	Cell signaling
Ep-CAM	ab71916	Abcam
β-actin	MAB1501	EMD Millipore

Table S3. Co-localization coefficient of CK19 and vimentin in small-for-size fatty grafts of rat or human.

		Weighted co-localization coefficient	
		Ch2 (green, CK19)	Ch1 (magenta, Vimentin)
Rat (n=3)	Day 7	0.52±0.19	0.32±0.18
	Day 14	0.28±0.10	0.37±0.15
Human (n=3)	6 M	0.92±0.08	0.58±0.25
	11 M	0.45±0.21	0.40±0.19

Co-localization analysis was performed by software ZEN. At each time points, 5 regions of interest in high power field for each sample were assessed. Data represent the mean ± SD.